MAY 11 1977

AEDC-TR-77-19

9.2

ROUGHNESS AND WALL TEMPERATURE EFFECTS ON BOUNDARY-LAYER TRANSITION ON A 0.0175-SCALE SPACE SHUTTLE ORBITER MODEL TESTED AT MACH NUMBER 8

VON KARMAN GAS DYNAMICS FACILITY
ARNOLD ENGINEERING DEVELOPMENT CENTER
AIR FORCE SYSTEMS COMMAND
ARNOLD AIR FORCE STATION, TENNESSEE 37389

April 1977

Final Report for Period 20 — 23 August 1976

TECHNICAL REPORTS
FILE COPY

PROPERTY OF U.S. AIR FORCE
AEDC TECHNICAL LIBRARY

Approved for public release; distribution unlimited.

Property of U. S. Air Force
AEDC LIBRARY
F40600-75-C-0001

Prepared for

NATIONAL AERONAUTICS AND SPACE ADMINISTRATION (JSC/EX33)
HOUSTON, TEXAS 77058

NOTICES

When U. S. Government drawings specifications, or other data are used for any purpose other than a definitely related Government procurement operation, the Government thereby incurs no responsibility nor any obligation whatsoever, and the fact that the Government may have formulated, furnished, or in any way supplied the said drawings, specifications, or other data, is not to be regarded by implication or otherwise, or in any manner licensing the holder or any other person or corporation, or conveying any rights or permission to manufacture, use, or sell any patented invention that may in any way be related thereto.

Qualified users may obtain copies of this report from the Defense Documentation Center.

References to named commercial products in this report are not to be considered in any sense as an endorsement of the product by the United States Air Force or the Government.

This report has been reviewed by the Information Office (OI) and is releasable to the National Technical Information Service (NTIS). At NTIS, it will be available to the general public, including foreign nations.

APPROVAL STATEMENT

This technical report has been reviewed and is approved for publication.

FOR THE COMMANDER

Chauncey D. Smith, Jr.

CHAUNCEY D. SMITH, JR.
Lt Colonel, USAF
Chief Air Force Test Director, VKF
Directorate of Test

Alan L. Devereaux

ALAN L. DEVEREAUX
Colonel, USAF
Director of Test

REPORT DOCUMENTATION PAGE		READ INSTRUCTIONS BEFORE COMPLETING FORM
1 REPORT NUMBER AEDC-TR-77-19	2 GOVT ACCESSION NO.	3. RECIPIENT'S CATALOG NUMBER
4. TITLE *(and Subtitle)* ROUGHNESS AND WALL TEMPERATURE EFFECTS ON BOUNDARY-LAYER TRANSITION ON A 0.0175-SCALE SPACE SHUTTLE ORBITER MODEL TESTED AT MACH NUMBER 8		5. TYPE OF REPORT & PERIOD COVERED Final Report, 20 - 23 August 1976 6. PERFORMING ORG. REPORT NUMBER
7 AUTHOR(s) G. D. Wannenwetsch and W. R. Martindale, ARO, Inc.		8. CONTRACT OR GRANT NUMBER(s)
9 PERFORMING ORGANIZATION NAME AND ADDRESS Arnold Engineering Development Center (XO) Air Force Systems Command Arnold Air Force Station, TN 37389		10. PROGRAM ELEMENT, PROJECT, TASK AREA & WORK UNIT NUMBERS Program Element 921E
11 CONTROLLING OFFICE NAME AND ADDRESS National Aeronautics and Space Administration (NASA-JSC/EX33), Houston, TX 77058		12. REPORT DATE April 1977 13. NUMBER OF PAGES 38
14 MONITORING AGENCY NAME & ADDRESS*(if different from Controlling Office)*		15 SECURITY CLASS. *(of this report)* UNCLASSIFIED 15a. DECLASSIFICATION DOWNGRADING SCHEDULE N/A

16. DISTRIBUTION STATEMENT *(of this Report)*

Approved for public release; distribution unlimited.

17 DISTRIBUTION STATEMENT *(of the abstract entered in Block 20, if different from Report)*

18 SUPPLEMENTARY NOTES

Available in DDC.

19. KEY WORDS *(Continue on reverse side if necessary and identify by block number)*

Space Shuttle
heat transfer
boundary-layer transition
reentry flight
wind tunnel tests
hypersonic flow

20. ABSTRACT *(Continue on reverse side if necessary and identify by block number)*

Heat-transfer tests were conducted on the Space Shuttle Orbiter Vehicle in the AEDC/VKF Hypersonic Wind Tunnel (B) to determine the location of boundary-layer transition for a simulated reentry phase flight profile. The model was a 0.0175-scale model with simulated randomly misaligned thermal protection system tiles etched into the windward surface. The tests were conducted at a nominal free-stream Mach number of 8, free-stream

DD FORM 1 JAN 73 1473 EDITION OF 1 NOV 65 IS OBSOLETE

20. ABSTRACT (Continued)

unit Reynolds numbers ranging from 0.5 million to 3.7 million per ft, and angles of attack of 30, 35, and 40 deg. Values of wall temperature to free-stream stagnation temperature (T_w/T_o) ranged from 0.14 to 0.44. A complete description of a liquid nitrogen cooling technique developed to produce low T_w/T_o values is presented. Representative test data and an analysis of the windward surface centerline heat-transfer data are included. Effects of wall temperature, tile roughness, and angle of attack on the location of transition are discussed.

AFSC
Arnold AFS Tenn

PREFACE

The work reported herein was conducted by the Arnold Engineering Development Center (AEDC), Air Force Systems Command (AFSC), at the request of the National Aeronautics and Space Administration, Johnson Space Center (NASA/JSC), Houston, Texas, under Program Element 921E. The results of the test were obtained by ARO, Inc., AEDC Division (a Sverdrup Corporation Company), operating contractor for the AEDC, AFSC, Arnold Air Force Station, Tennessee, under ARO Project Number V41B-K4A. The authors of this report were G. D. Wannenwetsch and W. R. Martindale, ARO, Inc. The final data package was completed on November 17, 1976, and the manuscript (ARO Control No. ARO-VKF-TR-76-146) was submitted for publication on December 17, 1976.

CONTENTS

ILLUSTRATIONS

Figure

Page

TABLES

1.0 INTRODUCTION

The location of boundary-layer transition on the windward surface of the Space Shuttle Oribiter during reentry is a critical factor in determining the surface heating rates experienced by the Orbiter thermal protection system (TPS). Two of the parameters which have been shown to affect transition location are wall-to-total temperature ratio and surface roughness. A series of tests was conducted in the von Kármán Gas Dynamics Facility (VKF) Hypersonic Tunnel (B) at Mach number 8 using a 0.0175-scale Orbiter model with the objective of independently varying these parameters to determine the effects on transition location.

The initial entry in the present series of tests (designated OH4A) used a smooth model. For this test, a new liquid nitrogen cooling technique was developed so that a model wall-to-total temperature ratio (T_w/T_o) of approximately 0.14 was achieved in addition to the normal ratio of 0.44, which is obtained by conventional high pressure air cooling. These temperature ratios provided a good duplication of expected flight values of approximately 0.05 to 0.2. The results of the OH4A test showed no significant change in transition location on the smooth model for the range of temperature ratios investigated.

The next test in this series (designated MH2A) investigated the effect of 0.001-in.-high simulated thermal protection system tiles that were plated on the model surface in a random manner to simulate roughness. At a temperature ratio of 0.44, there was no effect of the tile roughness on boundary-layer transition location. When an attempt was made to cool the model with liquid nitrogen, the tiles separated from the surface, causing termination of the test.

This report is primarily concerned with the third test in the series (designated MH2B). For this test, the model surface was etched away leaving 0.002-in.-high simulated tiles. Techniques were developed to obtain two additional wall-to-total temperature ratios between the extremes already mentioned, giving a total of four. Data are presented to show the effects of this wall-to-total temperature variation on transition location and also to illustrate the effects of Reynolds number (varied from 0.5×10^6 to 3.7×10^6 per ft) and angle of attack (30, 35, and 40 deg). Comparisons are also made with the data from the previous tests.

2.0 TEST ARTICLES

2.1 WIND TUNNEL

Tunnel B (Fig. 1) is a continuous, closed-circuit, variable density wind tunnel with an axisymmetric contoured nozzle and a 50-in.-diam test section. The tunnel can be

operated at a nominal Mach number of 6 or 8 at stagnation pressures from 20 to 300 and 50 to 900 psia, respectively, at stagnation temperatures up to 1,350°R. The model can be injected into the tunnel for a test run and then retracted for model cooling or model changes without stopping the tunnel flow. A description of the tunnel may be found in Reference 1.

2.2 MODEL

The model was a modified version of the 0.0175-scale Space Shuttle Orbiter configuration defined by Rockwell drawing VL70-000139 and designated model 29-0. A sketch of the model is shown in Fig. 2. The windward surface "finish" was modified in an effort to simulate randomly misaligned TPS tiles. To achieve the raised effect of the misaligned tiles, surrounding "unraised" areas of the model windward surface were etched away according to the following specifications:

1. Tile Pattern: Orientation of tiles in the centerline portion of the Orbiter as defined in Rockwell drawing VL70-399043 was used over the total area of interest.

2. Tile Area of Interest: The tile pattern began at 2 percent of the model length aft of the nose, covered the lower Orbiter area up to the tangent line of the chines and wing leading-edge thermal protection panels, and extended rearward to 80 percent of the model length.

3. Selection of Tiles to be Raised: Random selection of tiles was used to provide 25 percent raised tiles in the tile area of interest (see Fig. 3). Tiles were not etched within one tile length of any instrumentation or screw holes to permit polishing of instrumentation. The etched tile pattern was symmetrical about the model longitudinal centerline.

4. Tile Size: All selected tiles were etched to a height of approximately 0.002 in. (0.11 in., full scale). The tiles were 0.105 in. square (6 in. square, full scale).

Simulated surface gaps were machined into the model surface to simulate nose gear doors, forward external tank attach point, and wing leading edge thermal protection system tile joints. The model was supplied by the National Aeronautics and Space Administration, Johnson Space Center (NASA-JSC) and was constructed of 15-5 stainless steel. The raised tile surfaces were etched by Vought Systems Division of LTV, Dallas, Texas. There were no movable control surfaces on the model.

3.0 INSTRUMENTATION AND TEST PROCEDURES

3.1 INSTRUMENTATION

Coaxial surface thermocouple gages were used to measure the surface heating rate distributions. This type gage was chosen because of its unique construction features and its ability to function over the initial required temperature range (from -300 to 200°F). This type gage has been perfected in the VKF for use in the AEDC-VKF Hypervelocity Wind Tunnel (F) and has been used extensively for aerodynamic heating and transition studies (see Ref. 2). Its limitation is basically associated with finite gage length and the short allowable time for which this length can be exposed to a constant heat flux before semi-infinite solid theory becomes invalid.

The coaxial gage consists of an electrically insulated Chromel® center conductor enclosed in a cylindrical constantan jacket as shown in Fig. 4. After assembly and installation in the model, the gage materials are blended together with a jeweler's file. This results in thermal and electrical contact between the two materials in a thin layer at the surface of the gage (that is, a surface thermocouple). A second result of filing the gage surface is the opportunity for "perfect" contouring of the gage to the model surface. This fact was very important in the selection of coaxial gages since a smooth model surface is essential for transition studies. The model surface finish, including the gage surfaces, is estimated to have been between 20 and 50 microinches, with no measurable steps or gaps introduced by the gages. Sixty-nine gages were fabricated, calibrated, and installed by VKF personnel. Gage locations are given in Table 1.

The gage (thermocouple) outputs were recorded on magnetic tape using a Beckman 210 analog-to-digital converter. Each thermocouple output was sampled 20 times per second from the start of the model injection cycle until 3 sec after the model reached tunnel centerline.

This identical measuring and acquisition system was also used during the previous Tunnel B Orbiter heating tests MH-2A and OH4A.

3.2 TEST CONDITIONS

Nominal free-stream conditions at which the tests (MH2B) were conducted are given below, and the test summary is given in Table 2.

M_∞	P_o, psia	T_o, °R	HREF, Btu/sec-ft^2-°R	Re/ft x 10^{-6}
7.94	210	1,270	0.0244	1.0
7.97	325	1,295	0.0303	1.5
7.98	425	1,300	0.0345	2.0
7.98	545	1,310	0.0391	2.5
7.99	675	1,330	0.0436	3.0
8.00	860	1,340	0.0490	3.7

3.3 TEST PROCEDURE

Prior to each test run (or model injection into the flow) the model was cooled to an isothermal condition. Wall-to-stream total temperature ratios of 0.14, 0.24, 0.34, and 0.44 were provided by various methods of model cooling. The highest temperature ratio (T_w/T_o = 0.44, T_w = 545°R) was provided by the normal model cooling apparatus, which uses high pressure air jets. The lowest temperature ratio (T_w/T_o = 0.14, $T_w \approx$ 140°R) was obtained by spraying the model with jets of liquid nitrogen. Manifolds directed the cooling jets over the model windward surface. The tunnel tank pressure was maintained above the triple point pressure for nitrogen so that the liquid nitrogen sprayed on the model would remain in the liquid state. Cooling the model in this manner resulted in a reasonably uniform initial surface temperature (T_w) of about 140°R. Data at intermediate wall temperatures were produced using various mixtures of liquid and gaseous nitrogen and by decreasing tank pressure below the triple point, thus cooling with nitrogen "snow".

Two basic problems related to the liquid nitrogen cooling were encountered. The liquid nitrogen cooling effects on the model support hardware were quite severe, and occasionally it was necessary to stop cooling and allow the equipment to warm up. A problem which was critical to the success of the test was the frost accumulation on the model. The wind tunnel air is relatively dry; however, when the model temperature dropped below the frost point (approximately -30°F at atmospheric pressure), a thin layer of frost began to form. To control this problem the nitrogen was allowed to flow continuously, thus effectively blanketing the model in a dry nitrogen atmosphere. For a test run the model was injected into the airstream out of this nitrogen blanket; as a result the model experienced only a limited exposure to the relatively humid air environment. The cold model caused the water vapor in the air to form a frost layer, and after every

third run the model was warmed to room temperature to remove the frost accumulation. This procedure produced satisfactory results with only a light haze appearing on the model during a test run. For a few runs the frost was thicker than usual, and these runs are noted in the test summary, Table 2.

3.4 DATA REDUCTION

The coaxial gage provides measurement of the surface temperature of the gage-model composite, which is assumed to be a homogeneous, one-dimensional, semi-infinite solid. Of course, the gages and model skin are of finite thickness (about 0.3 in.), and the semi-infinite solid assumption is valid for a maximum of about 2 sec. However, this time is adequate for data acquisition, and the above assumptions are used to compute the heat flux at the model surface.

For one-dimensional heat flow into a semi-infinite solid, the surface temperature difference, $\overline{T}(t)$, and the surface heat flux, $\dot{q}(t)$, are related by the following expression (Ref. 3):

$$\dot{q}(t) = \frac{\left(\rho c_p k\right)^{1/2}}{\pi^{1/2}} \left[\frac{\overline{T}(t)}{t^{1/2}} + \frac{1}{2} \int_0^t \frac{\overline{T}(t) - \overline{T}(\tau)}{\left(t - \tau\right)^{3/2}} \, d\tau \right] \tag{1}$$

where τ is a dummy time variable of integration and T equals $T_w - T_{w_i}$. Cook and Felderman (Ref. 4) have developed a numerical technique for the solution of this equation which does not involve assumptions about the nature of the input function. Their result was modified to produce a shorter form for the numerical expression. This modification involved algebraic manipulations and did not involve changing the basic assumptions of the problem. The final equation is shown below.

$$\dot{q}(t) = \frac{\left(2 \rho c_p k\right)^{1/2}}{\sqrt{\pi}} \sum_{i=1}^{\eta} \left[\frac{\overline{T}(t_i) - \overline{T}(t_{i-1})}{t_i - t_{i-1}} \left(\sqrt{t_\eta - t_{i-1}} - \sqrt{t_\eta - t_i} \right) \right] \tag{2}$$

This expression was used in the present data reduction procedure.

The solution of Eq. (2) is affected by noise in the thermocouple signal which is used to compute $\overline{T}$. To reduce noise effects and improve accuracy in the final result, values of $\dot{q}(t)$ were averaged over a period of one second after the model reached tunnel centerline. The average value of surface temperature over this period was used to calculate the heat-transfer coefficients.

The evaluation of Eq. (2) requires a value for the lumped thermal parameter $(\rho c_p k)^{1/2}$. Since the gages are a composite of Chromel and constantan, an effective value of $(\rho c_p k)^{1/2}$ for the gages must be used. The properties for these materials are nearly equal at room temperature but differ substantially at low temperatures (such as -300°F). Prior to the OH4A test in Tunnel B, the values of $(\rho c_p k)^{1/2}$ were determined experimentally at three temperatures (liquid nitrogen, 150°R; dry ice, 390°R; and ambient air, 545°R). The results are shown in Fig. 5, which indicates a linear relationship over the temperature range of interest. The slope of the linear equation shown was used in the data reduction for the $(\rho c_p k)^{1/2}$ values. The intercept of the equation was adjusted for each individual gage by calibrating each gage at room temperature prior to testing.

4.0 DATA PRECISION

4.1 TEST CONDITIONS

Uncertainties of the basic tunnel parameters were estimated from repeat calibration of the P_o and T_o instruments and from the repeatability and uniformity of the tunnel flow during calibrations. The parameters P_o, T_o, and M_∞, with their uncertainties, were then used to compute the uncertainty in Reynolds number per foot by means of the Taylor series method of error propagation.

Uncertainty, percent			
M_∞	P_o	T_o	Re/ft
±0.3	±0.5	±0.5	±1.2

4.2 HEAT-RATE MEASUREMENTS

The coaxial heat gage is assumed to be a homogeneous, one-dimensional, semi-infinite solid. However, since the gage has a finite length, the semi-infinite slab solution for the gage surface temperature response is valid only for a short period of time. An evaluation of the errors in the measured heating rates caused by the gages' finite depth was made by comparing semi-infinite with finite slab solutions for an exposure time on the order of the actual test data (that is, approximately 2 sec). Use of gage material thermophysical properties at room temperature resulted in comparisons which indicated that the semi-infinite solution produced results from 0 to approximately 3 percent too high. For liquid nitrogen temperature gage properties, the semi-infinite solutions gave values up to 25 percent high. Since the primary test objective was to locate boundary-layer transition, an error in the absolute level of heating rate of the magnitude indicated was not considered serious.

A statistical analysis of the data from several gages was made to determine the consistency of the data within a test run. Data system noise and data reduction effects on the results were thus obtained. The results are shown below.

q, Btu/ft^2-sec	Uncertainty,* percent
5 or greater	7
1	10
0.5	25

*Uncertainty represents two standard deviations, which includes 95 percent of the data.

The estimated precision of the $(\rho c_p k)^{1/2}$ calibrations performed by the VKF is ±5 percent at room temperature. This translates to a ±10 percent uncertainty at liquid nitrogen temperatures. This estimate is based on repeatability of the results and periodic checks of the reference standards.

Combination of errors produced by data system noise and calibration uncertainties yields the estimated total uncertainty shown below:

	Total Uncertainty, percent	
q, Btu/ft^2-sec	Room Temperature	150°R
5 or greater	9	12
1	11	14
0.5	25	27

Individual gage calibrations were not performed for the OH4A and MH2A tests. A mean value from a single gage was used. This resulted in an estimated uncertainty of ±10 percent in $(\rho c_p k)^{1/2}$ at room temperatures and ±20 percent at liquid nitrogen temperatures.

5.0 RESULTS AND DISCUSSION

The primary result obtained in the OH4A, MH2A, and MH2B test series was the determination of boundary-layer transition locations at various test conditions. The interpretation of heating rate data for the purpose of locating transition requires some

judgement and, more importantly, a basis for comparison. Ideally, this basis is a known laminar heating rate distribution along the surface of interest. The beginning of transition is then determined by the demarcation of the data from the laminar values. The laminar heating rate distribution which was used as a basis for model centerline data analysis in this report was obtained using OH4A, MH2A, and MH2B data for a wall-to-total temperature ratio of 0.44 at a model angle of attack of 30 deg as shown in Fig. 6. The fairing of these data will be used as the laminar reference curve in the analysis of the transition locations.

5.1 MODEL COOLING TECHNIQUE

One primary objective of the OH4A, MH2A, and MH2B test series was to acquire data at model wall temperatures much lower than those attained using standard test techniques. The basis for the low temperature requirement is that estimated flight values of T_w/T_o are well below those ordinarily obtained during standard wind tunnel testing. Figure 7 illustrates this point. In the left-hand portion of Fig. 7, the standard operating limits in AEDC-VKF Hypersonic Wind Tunnels (B) and (C) are shown. These range estimates are based on model cooling with high pressure air at near ambient temperature for maximum tunnel stagnation temperatures. Flight values for T_w/T_o shown were calculated for conditions set forth in Rockwell International SSV Trajectory number 14,040 (Table 3). It is obvious that by attaining values of T_w/T_o in the neighborhood of 0.14 with the liquid nitrogen cooling technique (Section 3.3) a better simulation of T_w/T_o is obtained. As will be shown later in this section, a reduction in model wall temperature can have a profound influence on boundary-layer transition.

Model frost can become a significant parameter in test results obtained at very low model wall temperatures. To provide a dramatic comparison of frost effects, data were obtained at low wall temperature with "heavy" frost intentionally permitted to develop on the model prior to injection. The results of this investigation, as shown in Fig. 8a, indicate that the frost layer tended to delay boundary-layer transition and to give slightly lower heating levels ($\approx$ 15 percent below fairing). The downstream shift of the transition location with increasing frost thickness was the direct result of the frost's reducing the effectiveness of the surface tile roughness.

A study of frost influence on laminar heat-transfer-rate levels (Fig. 8b) reveals that a heavy frost accumulation may reduce measured heating levels by as much as 30 percent. As expected, a moderate frost level will also reduce heat-transfer levels, but to a lesser degree.

Frost levels were monitored visually throughout the test entries. The frost was generally maintained at a level no heavier than a slight haze.

5.2 WALL TEMPERATURE EFFECTS ON A SMOOTH WALL MODEL

One objective of the OH4A test entry was to determine the effect of model wall temperature variation on the location of transition without simulated tile roughness (that is, on a smooth wall model). Some typical OH4A results are presented in Fig. 9 and show no significant dependence of transition location on wall temperature ratio between 0.14 and 0.44 on the smooth wall model.

5.3 ROUGHNESS EFFECTS

Of major concern is the windward surface roughness (which can not be avoided in application of the TPS tiles) on the actual orbiter flight vehicle. The MH2A and MH2B test entries were designed to investigate what influence these misalignments could have on transition location during orbiter reentry.

A comparison of typical test data obtained during the OH4A, MH2A, and MH2B entries is presented in Fig. 10. Figure 10a shows that a negligible change in the location of the beginning of transition was produced by a variation in the height of the misaligned TPS tiles at warm model wall temperature ratio (T_w/T_o = 0.44). There was, however, a noticeable change in the transitional heating distribution. The T_w/T_o values obtained for this data are typical of those obtained during "standard" wind tunnel operation.

Investigation of the roughness effect at cold model wall temperature ratios (T_w/T_o = 0.14) conducted in the present tests produced significant effects of tile roughness on the location of transition. TPS tile misalignment becomes significantly more effective in promoting boundary-layer transition at the cold wall condition, as shown in Fig. 10b. In Fig. 10a, for instance, a cold wall, smooth model produced transition beginning at about 55 percent of the model length, while the roughened model at similar test conditions produced transition beginning at approximately 10 percent of model length (Fig. 10b).

The roughened, cold wall results examined above point out a problem that could arise when "standard" wind tunnel data obtained at T_w/T_o = 0.44 are applied to flight aerodynamic estimates. Because previous wind tunnel testing (which has been very extensive) has not included investigation of distributed roughness, wall temperature, or the interaction of these two parameters, an error of as much as 45 percent of the vehicle length in the estimation of transition location is possible.

5.4 SUMMARY OF TEST RESULTS

Figure 11 presents a summary of some of the transition location data. Data plots in Fig. 11 present transition location (X_t/L) and transition Reynolds number (Re_{X_t}) variation with free-stream unit Reynolds number. In Fig. 11a, the effects of wall temperature from the rough-surfaced MH2B test are presented. Wall-to-total temperature ratios of 0.44 and 0.34 yielded identical results at all free-stream conditions tested. However, the cold wall (T_w/T_o = 0.14) data consistently reveal a significant forward shift of transition as compared to the warmer wall temperature (T_w/T_o = 0.34 and 0.44) location. The low intermediate wall temperature (T_w/T_o = 0.24) produced a transition location in the region between the cold and warm wall results. Figure 11a makes it clear that these results apply over the entire range of Reynolds number tested.

Figure 11b demonstrates the effects of surface roughness for T_w/T_o values of 0.14 and 0.44. This figure shows that under warm wall conditions, the location of transition is essentially unchanged with variations in surface roughness height. The cold wall smooth surface data, although showing a slight downstream transition location trend, closely approximate the warm wall results. The cold wall data obtained with surface roughness heights of 0.002 in. show a transition location which is consistently upstream of the warm wall location by approximately 35 percent of the vehicle length.

Figure 11c illustrates the effect of angle-of-attack variation at cold, rough wall conditions. It should be obvious from Fig. 11c that the effect of angle of attack over the 30- to 40-deg range tested was small.

5.5 SAMPLE OF OFF-CENTERLINE DATA

Data were also obtained at various spanwise locations. A sample presentation of these data is shown in Fig. 12 for data obtained at the 60-percent wing semispan location. This figure shows an upstream movement of transition with decreasing wall temperature for the rough wall model. This is similar to trends found on the model centerline.

6.0 CONCLUSIONS

A series of wind tunnel tests was run at M_∞ = 8 on a 0.0175-scale model of the Space Shuttle Orbiter to determine the influence of various parameters on the location of boundary-layer transition. Of primary interest were the effect of variation of model wall temperature and model surface roughness. Wall-to-total temperatures from 0.14 to 0.44 were tested on models with distributed roughness heights of 0, 0.001, and 0.002 in. Other test variables included free-stream Reynolds number and model angle of attack. As

a result of investigations of these data as presented in the body of this report, the following conclusions may be drawn:

1. A reliable and efficient testing capability was developed which allows transition testing at T_w/T_o values as low as 0.14 with repeatable results.

2. The interaction of flight vehicle values for T_w/T_o = 0.14 and thermal protection system (TPS) tile misalignment can produce a shift in transition location on the Space Shuttle Orbiter of as much as 45 percent of the vehicle length when compared to results from standard warm wall, T_w/T_o = 0.44 smooth surface wind tunnel tests.

3. Variations in model angle of attack have very little effect on transition location.

REFERENCES

1. Test Facilities Handbook (Tenth Edition). "Von Kármán Gas Dynamics Facility, Vol. 3." Arnold Engineering Development Center, May 1974.

2. Pate, S. R. and Eaves, R. H. Jr. "Recent Advances in the Performance and Testing Capabilities of the AEDC-VKF Tunnel F (Hotshot) Hypersonic Facility." AIAA Paper No. 74-84, February 1974.

3. Carslaw, H. S. and Jaeger, J. C. Conduction of Heat in Solids. Second Edition, Oxford, Clarendon Press, 1959.

4. Cook, W. J. and Felderman, E. J. "Reduction of Data from Thin-Film Heat-Transfer Gages: A Concise Numerical Technique." AIAA Journal, Vol. 4, No. 3, March 1966.

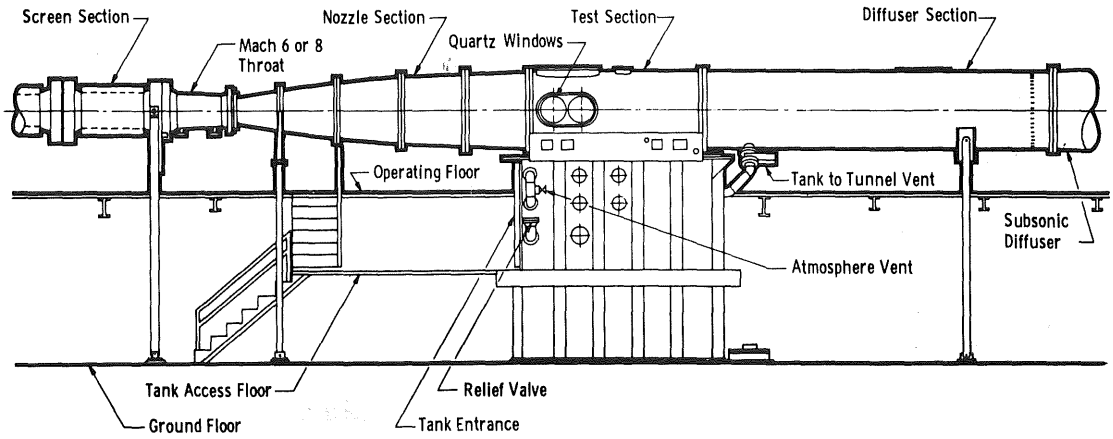

a. Tunnel assembly

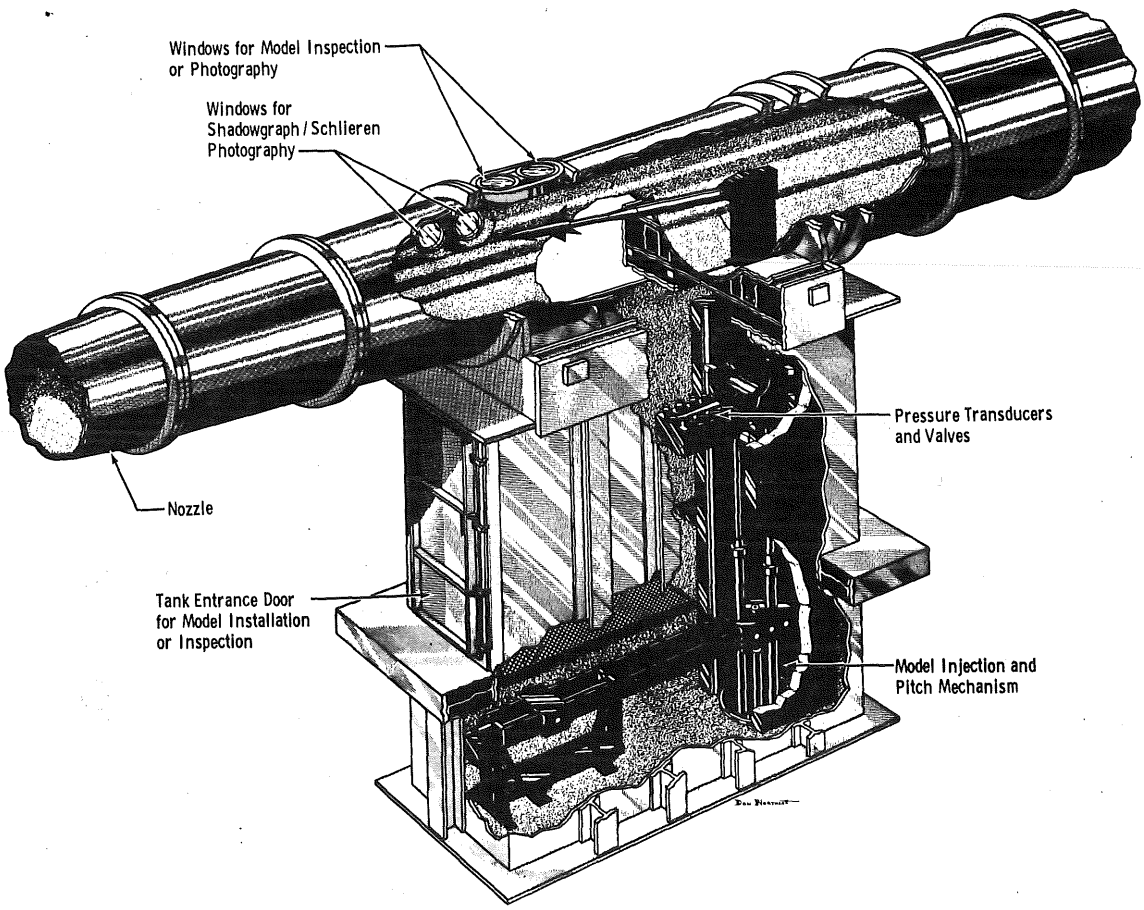

b. Tunnel test section

Figure 1. Tunnel B.

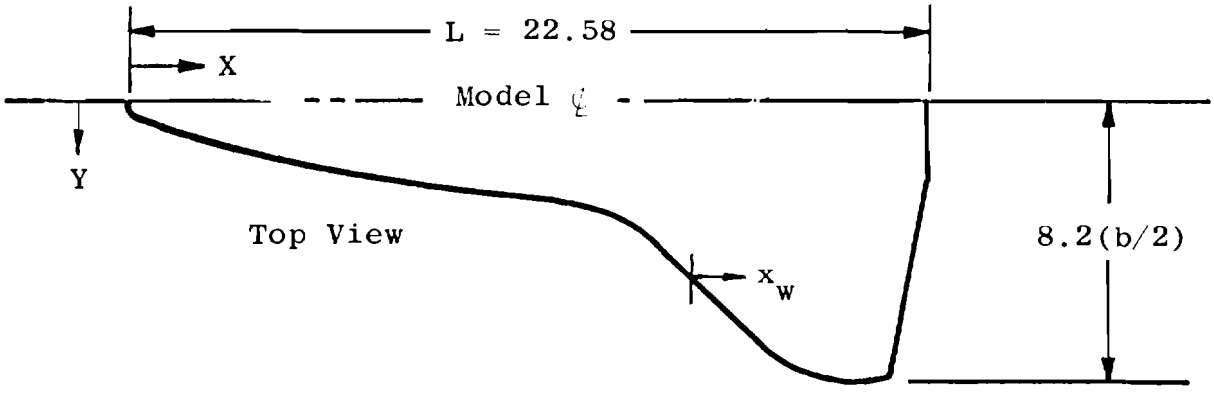

Dimensions are nominal
values in inches.

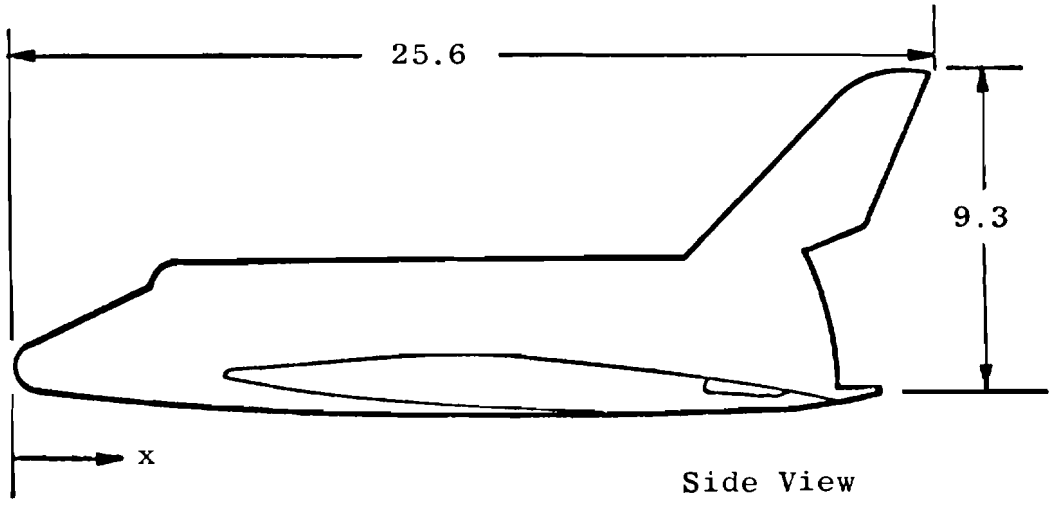

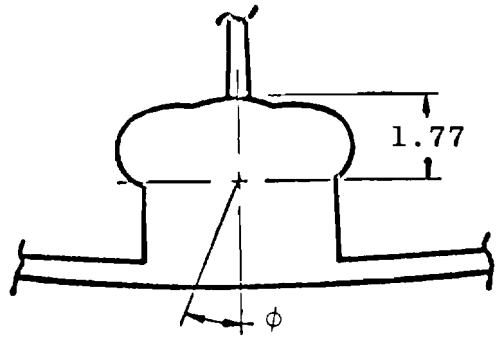

Rear View

Figure 2. Model.

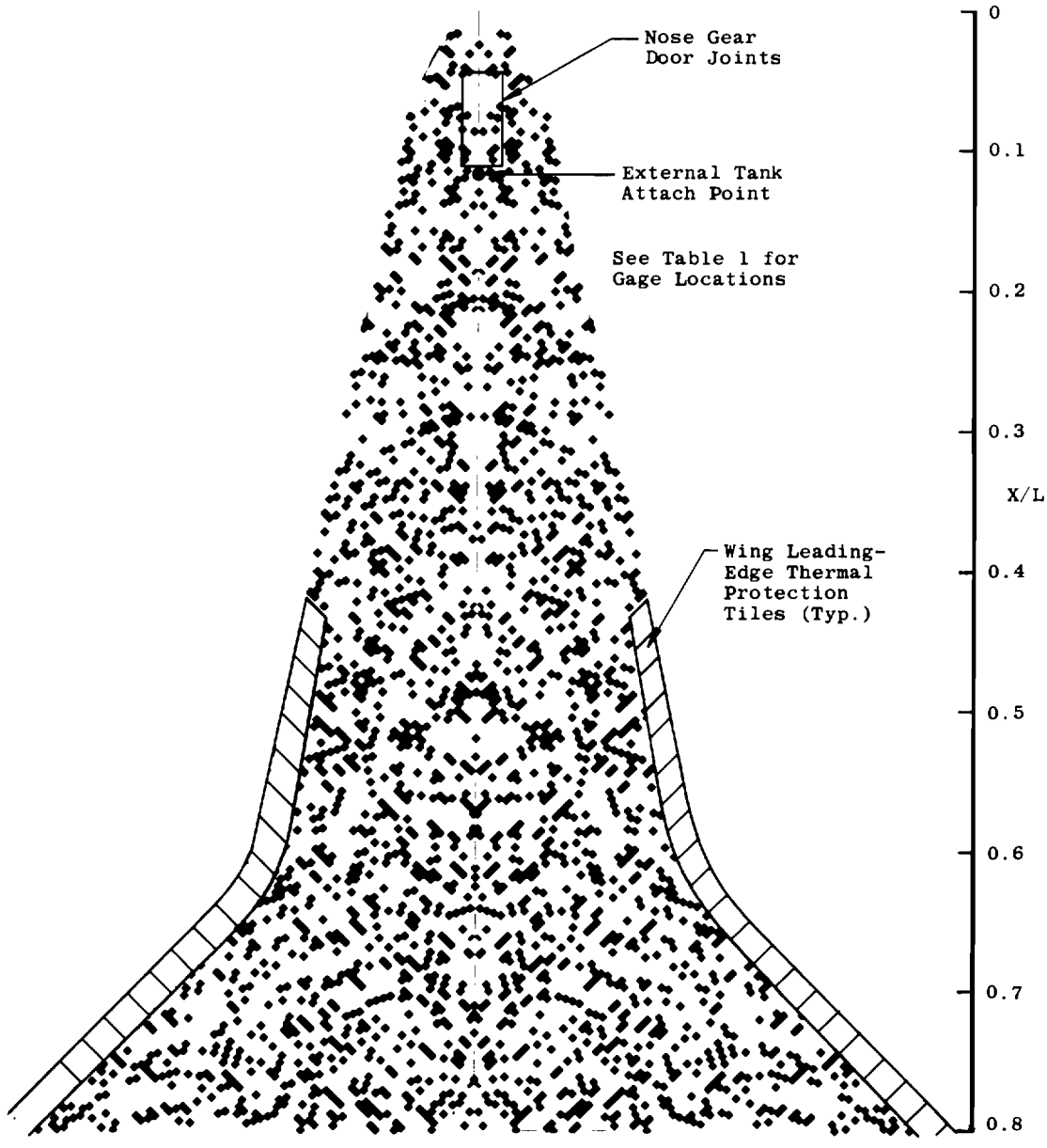

Figure 3. Orbiter thermal protection system tile misalignment pattern.

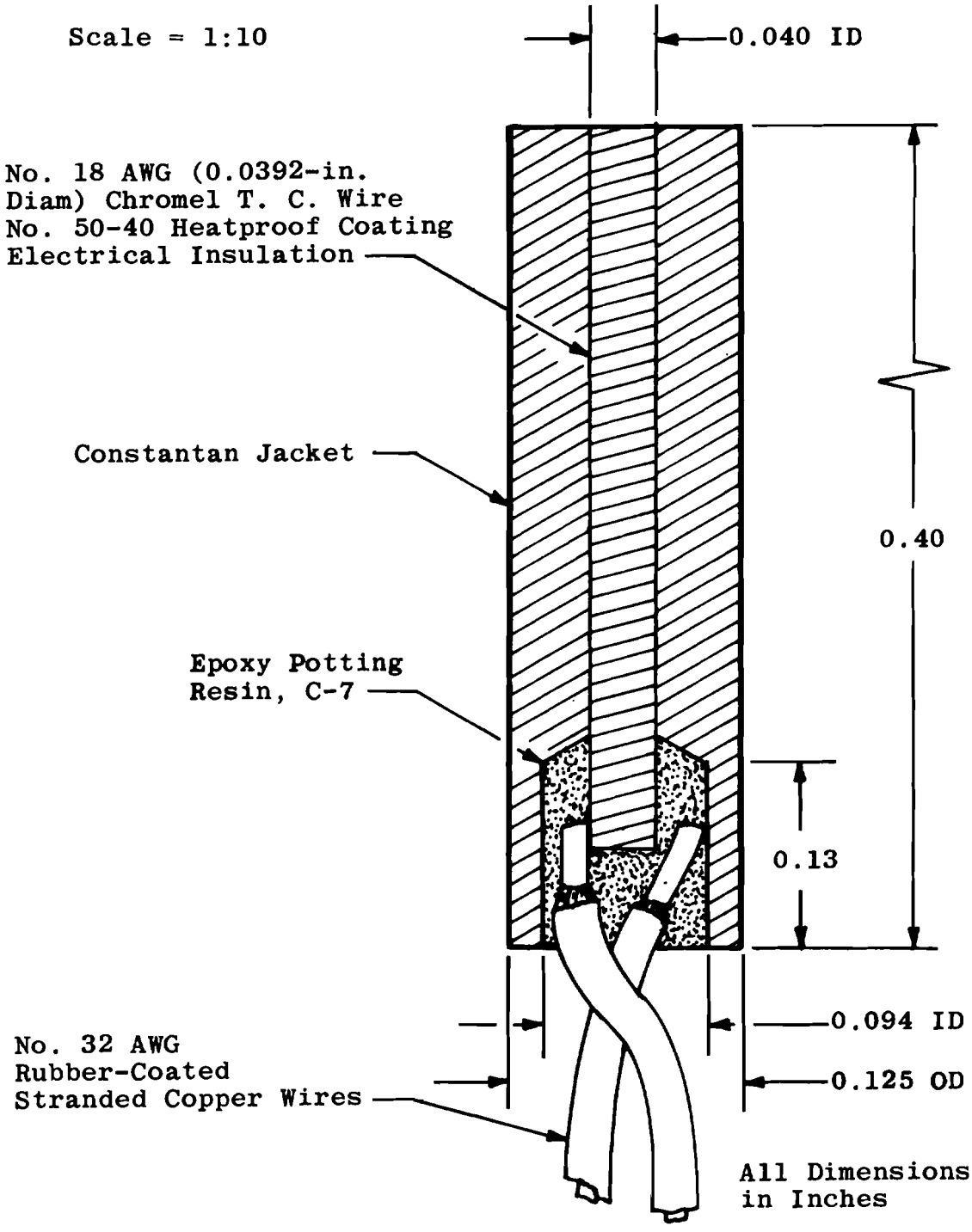

Figure 4. Chromel-constantan coaxial surface thermocouple gage.

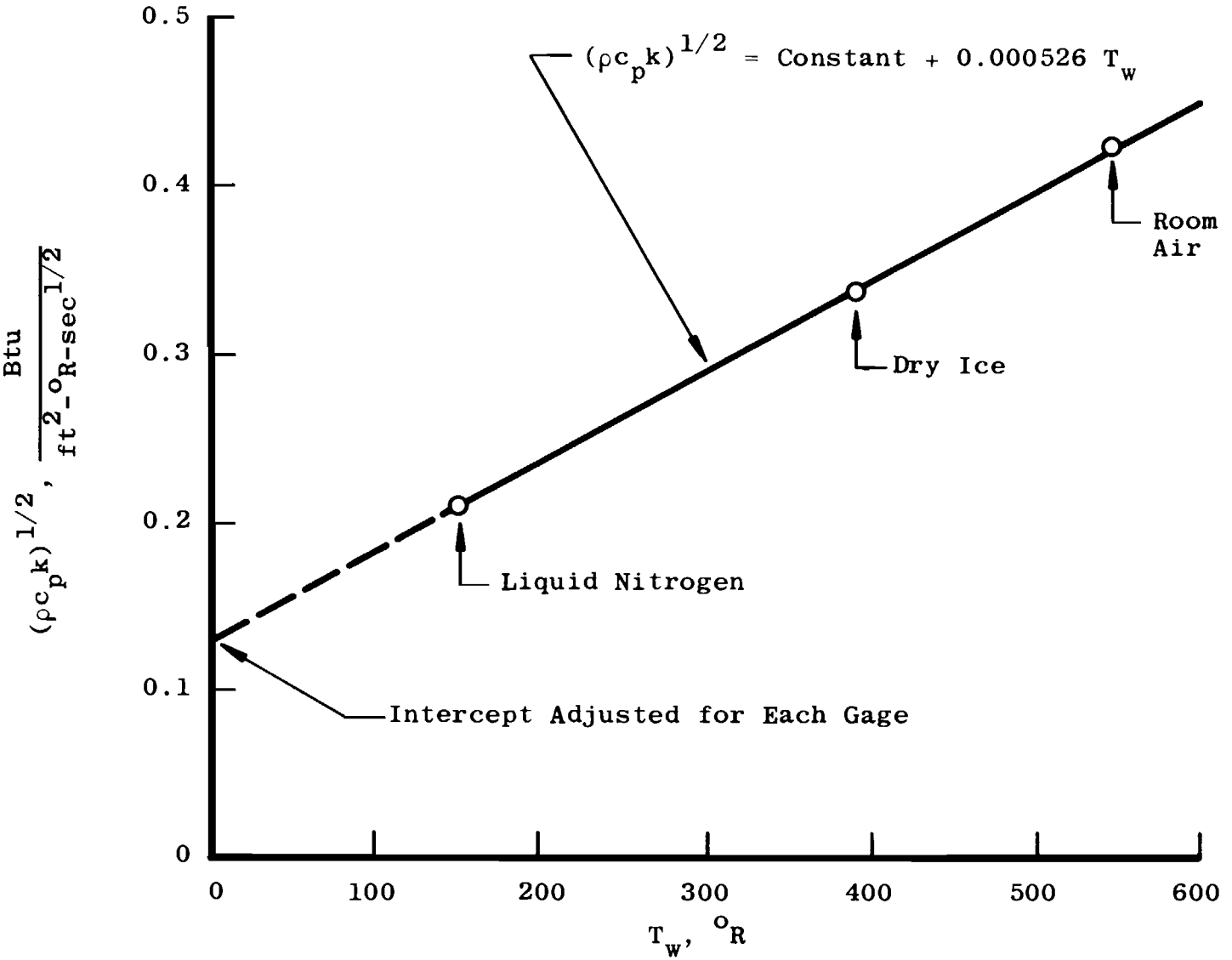

Figure 5. Gage thermal property calibration.

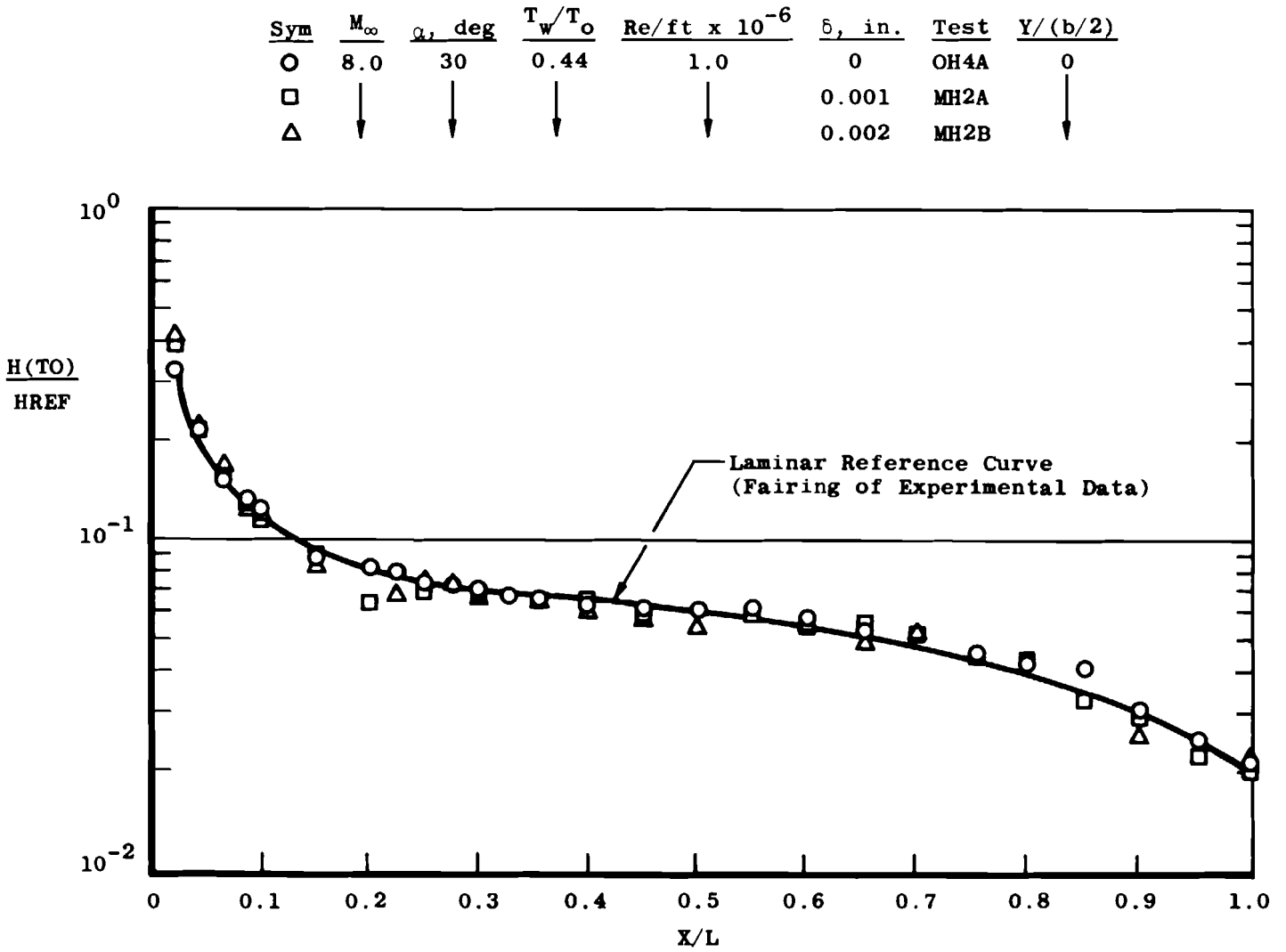

Figure 6. Laminar reference data.

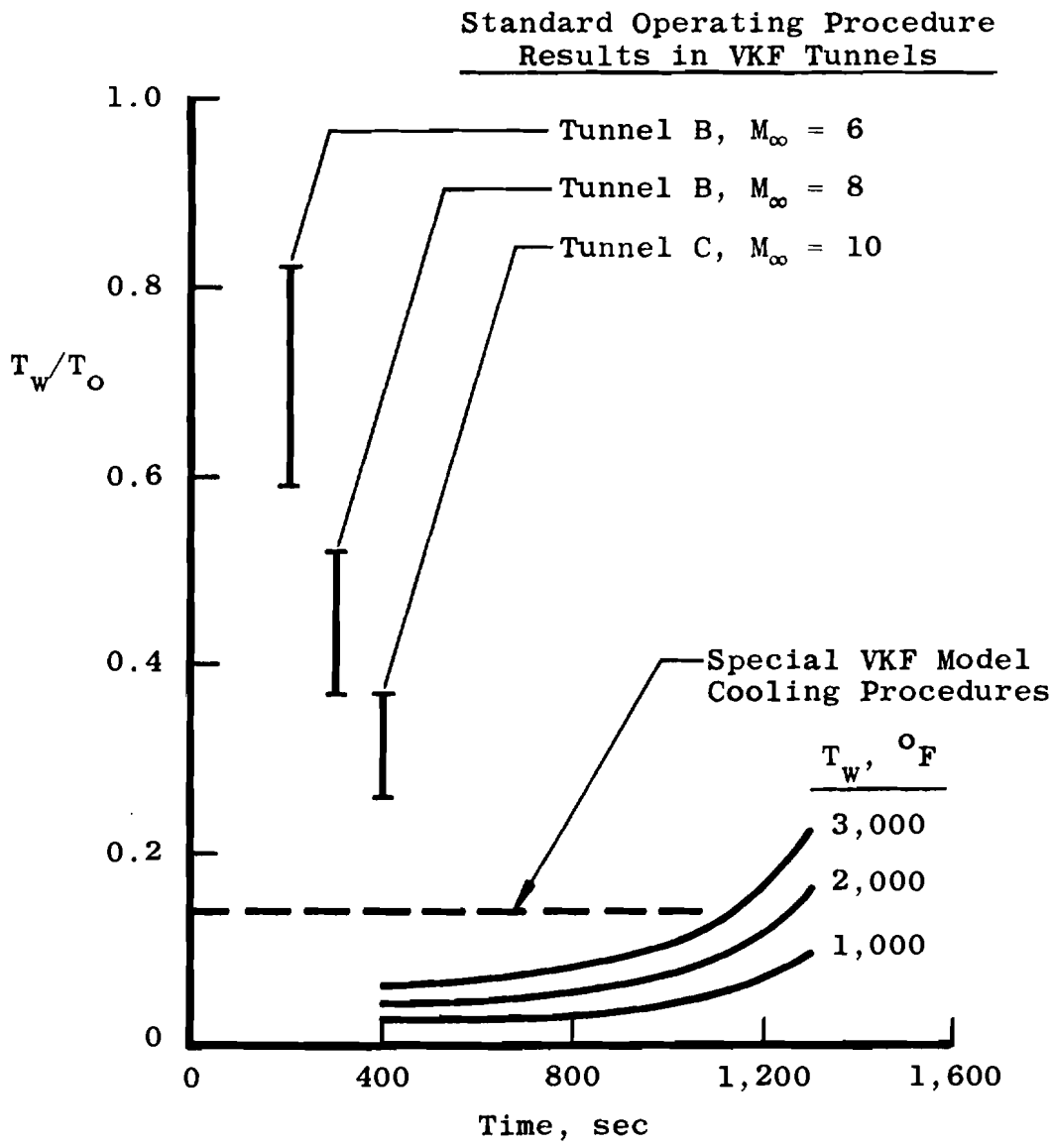

Figure 7. T_w/T_o calculated for Rockwell International SSV Trajectory No. 14,040.

Sym	M_∞	α, deg	T_w/T_o	Re/ft x 10^{-6}	δ, in.	Test	Y/(b/2)	Frost
○	8.0	30	0.14	3.7	0.002	MH2B	0	Heavy
□	8.0	30	0.14	3.7	0.002	MH2B	0	Std Test Level

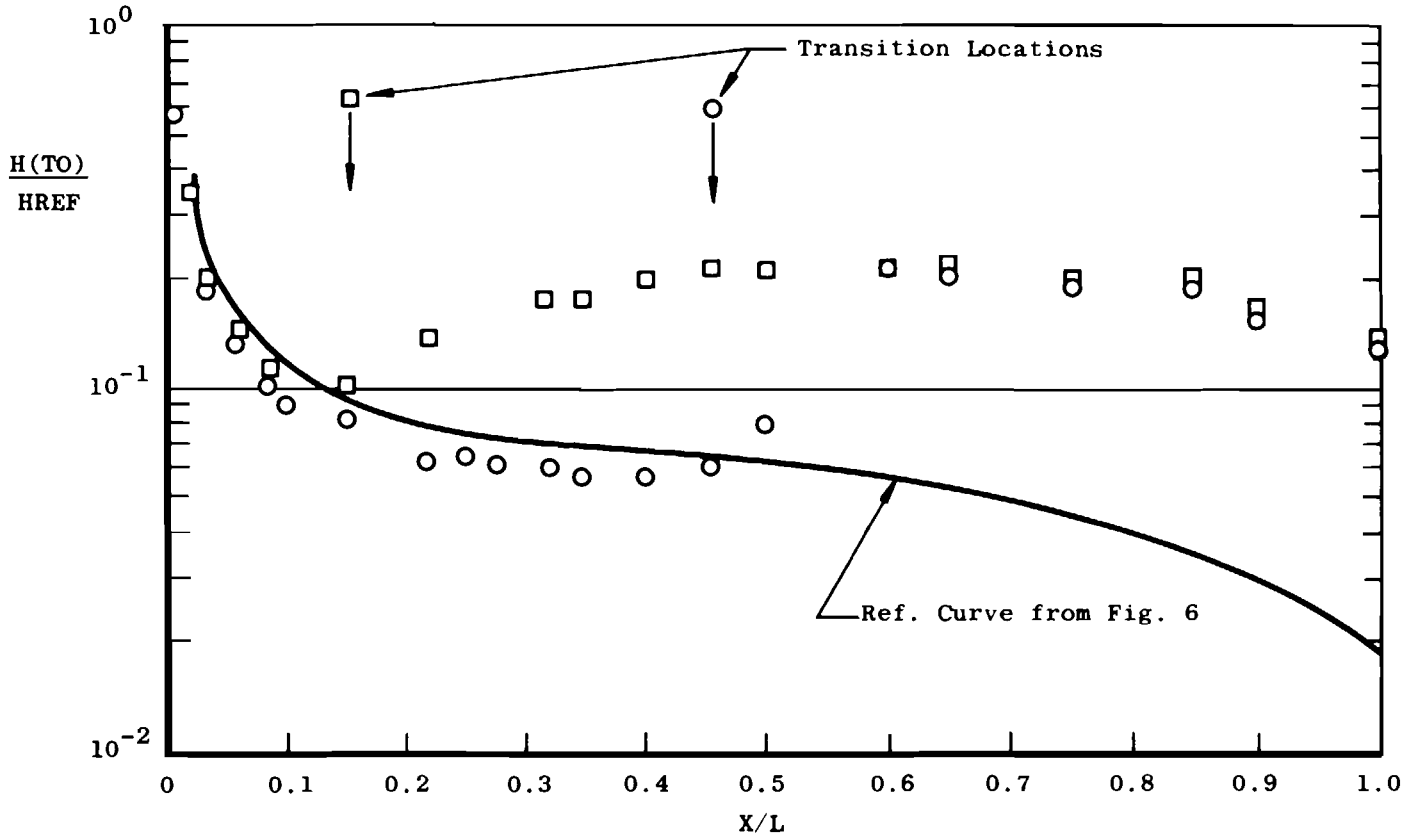

a. Frost effect on transition location

Figure 8. Frost effects on typical test data.

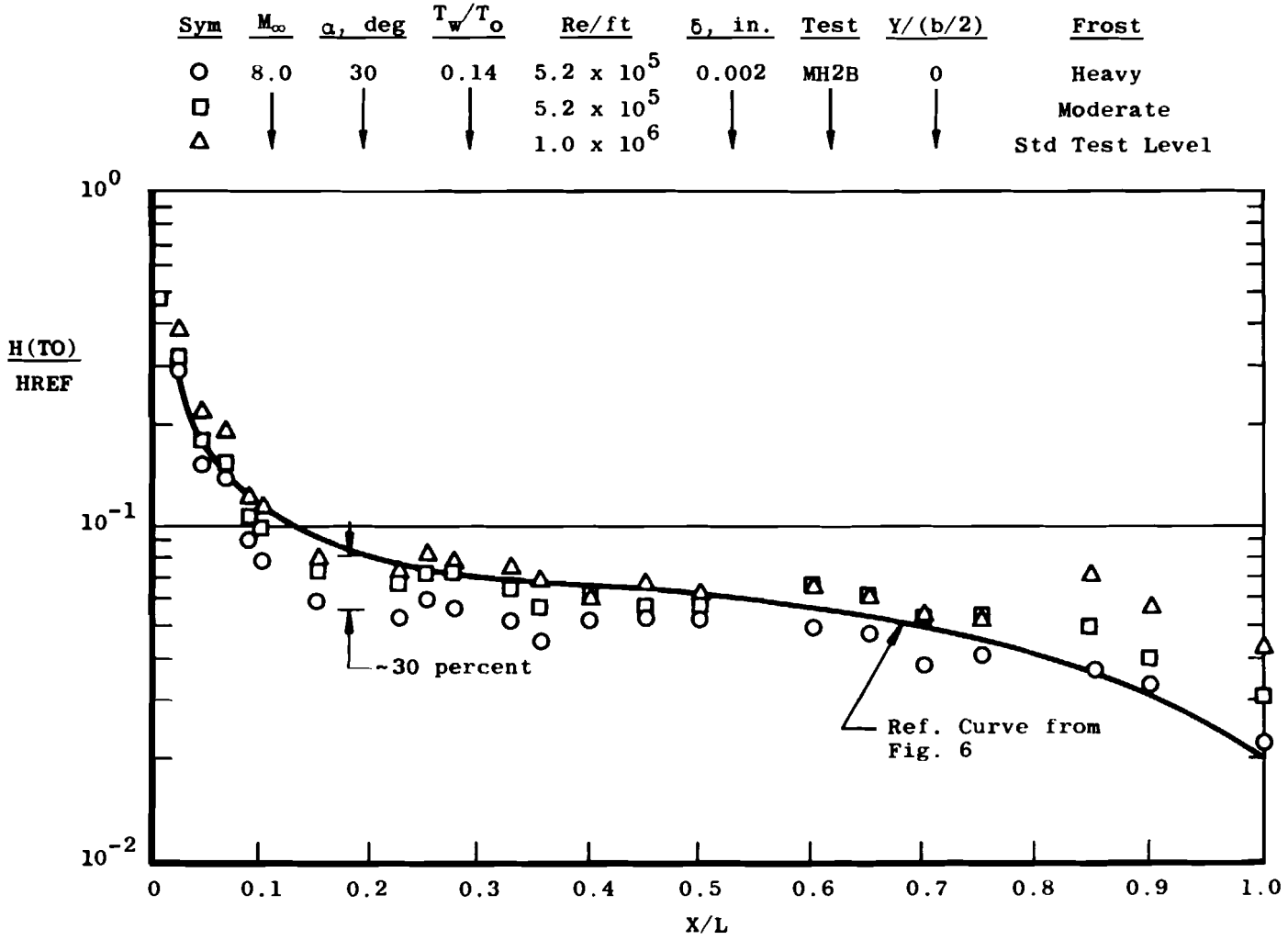

b. Frost effect on laminar heating levels
Figure 8. Concluded.

Sym	M_∞	α, deg	T_w/T_o	Re/ft x 10^6	δ, in.	Test	Y/(b/2)
○	8.0	30	0.44	3.7	0	OH4A	0
□	8.0	30	0.14	3.7	0	OH4A	0

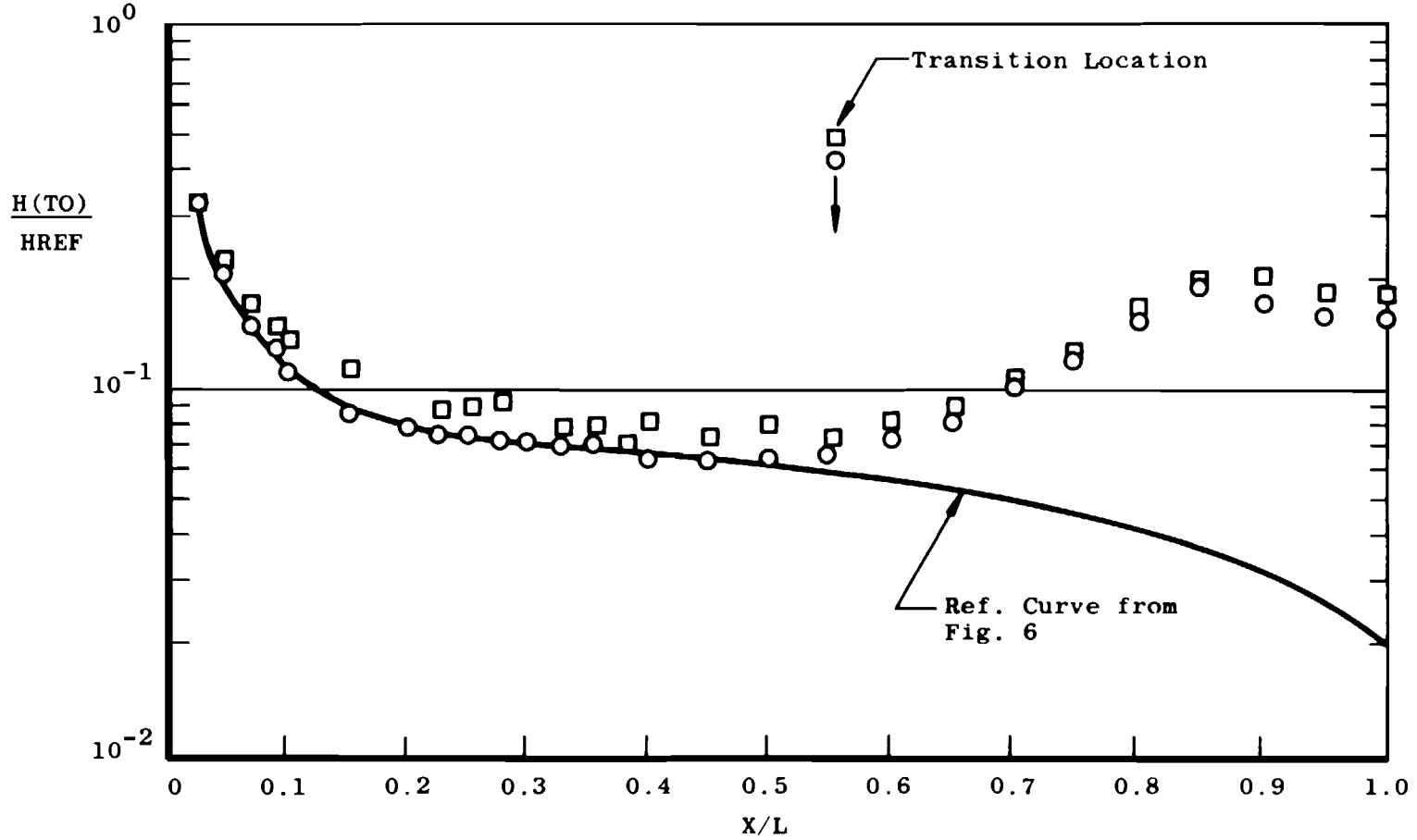

Figure 9. Wall temperature effect on transition location, δ = 0.

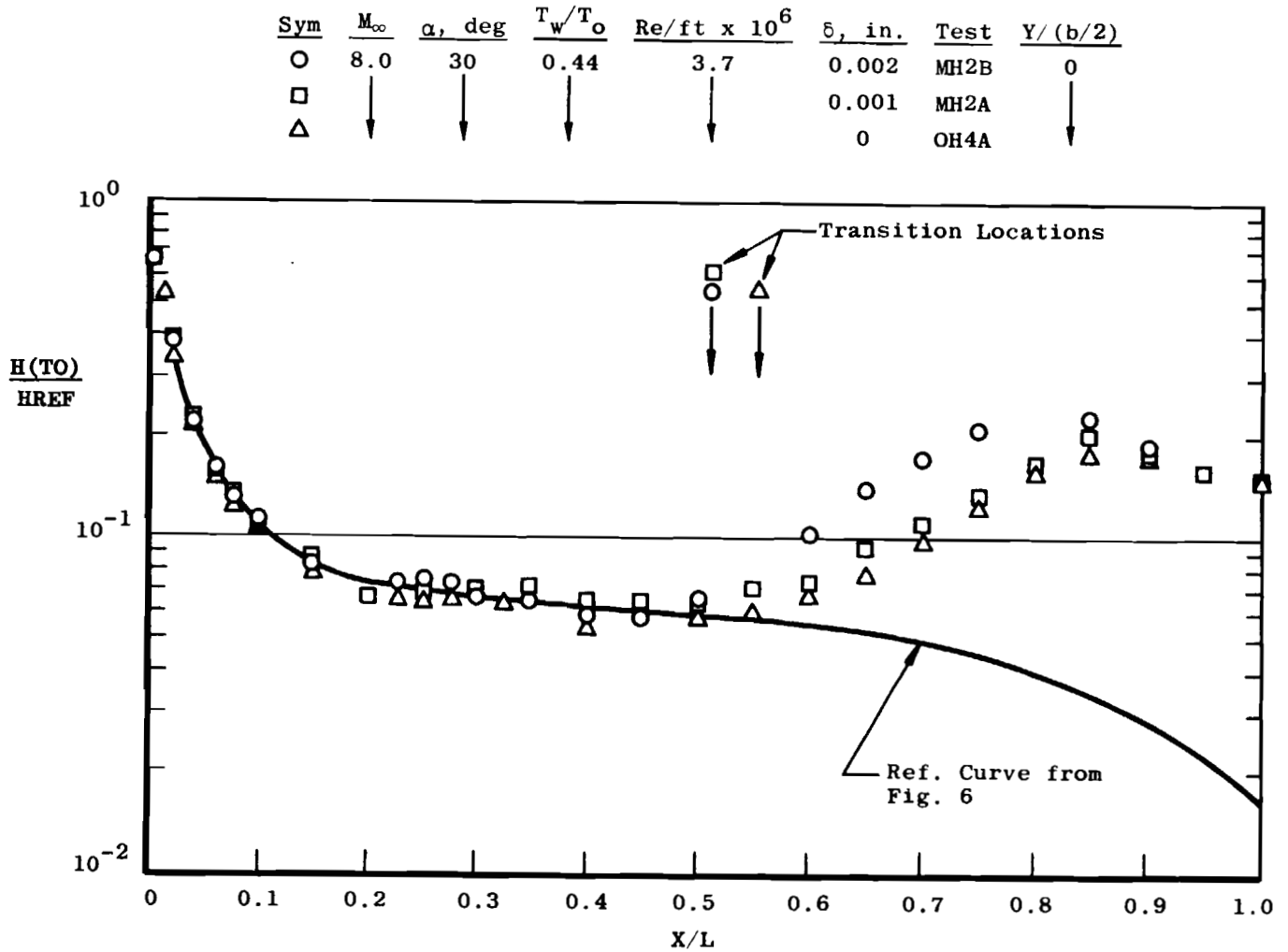

a. Warm wall conditions

Figure 10. Effects of TPS tile height on transition location.

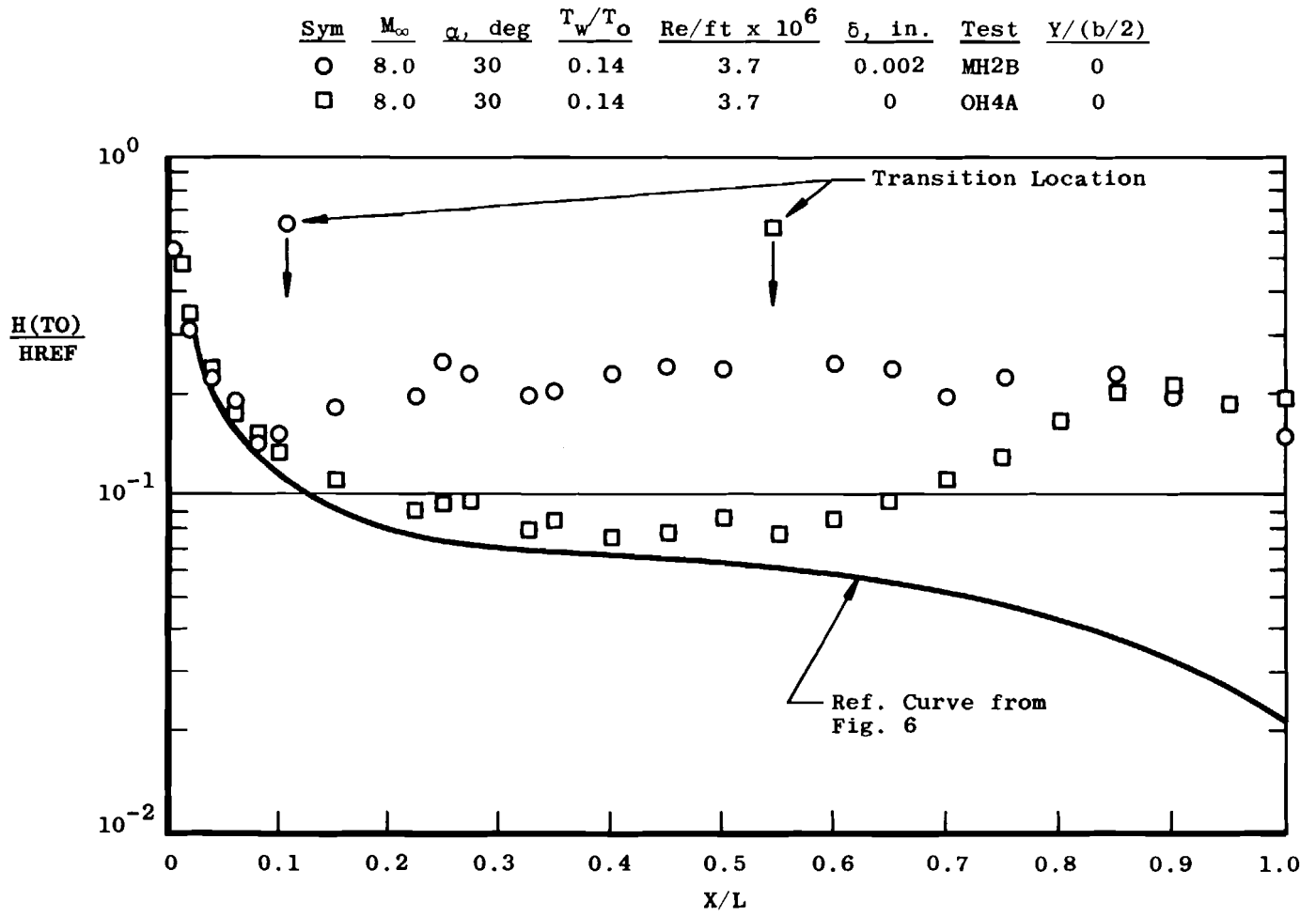

b. Cold wall conditions

Figure 10. Concluded.

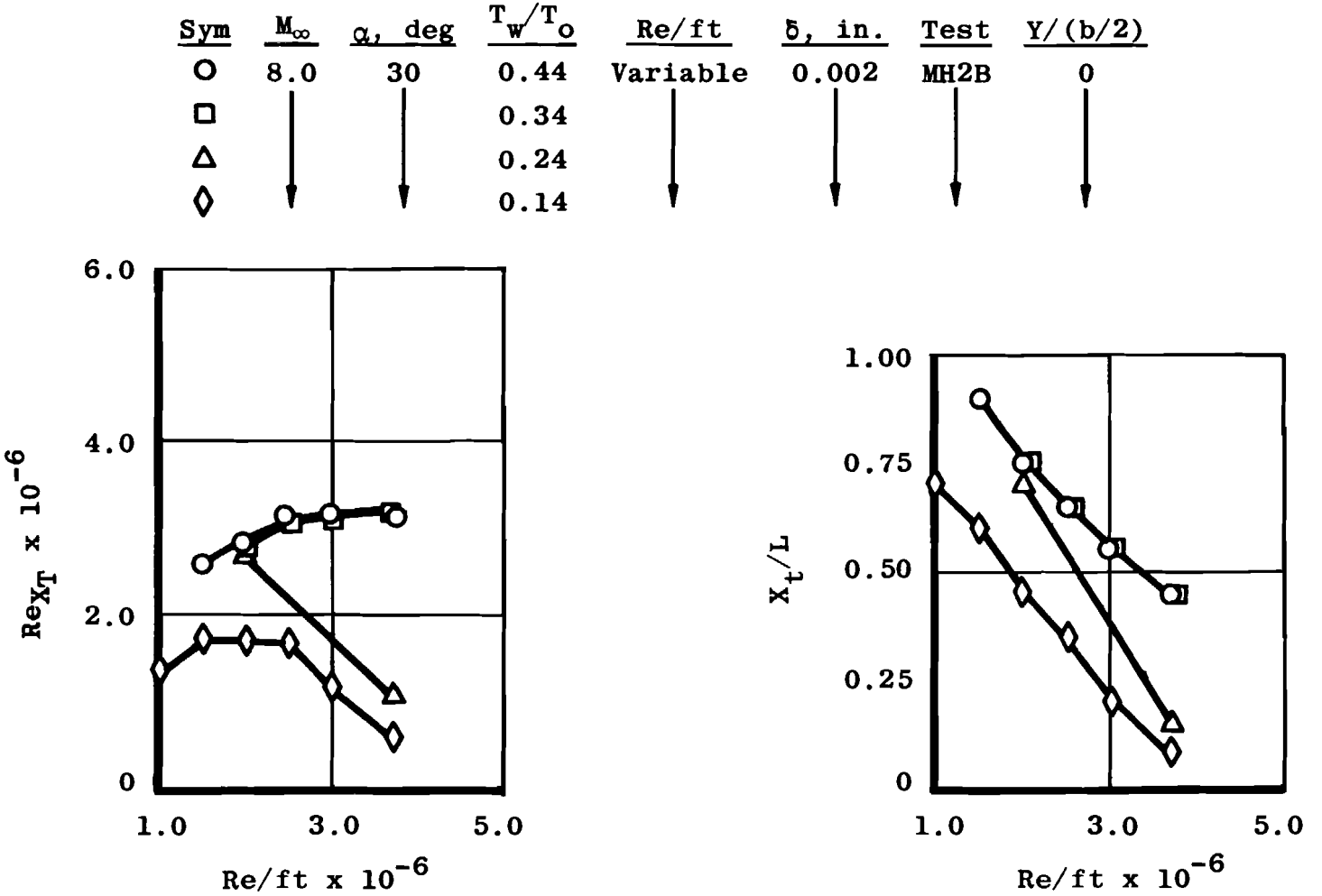

a. Wall temperature effects

Figure 11. Summary of wall temperature, surface roughness, and angle-of-attack effects.

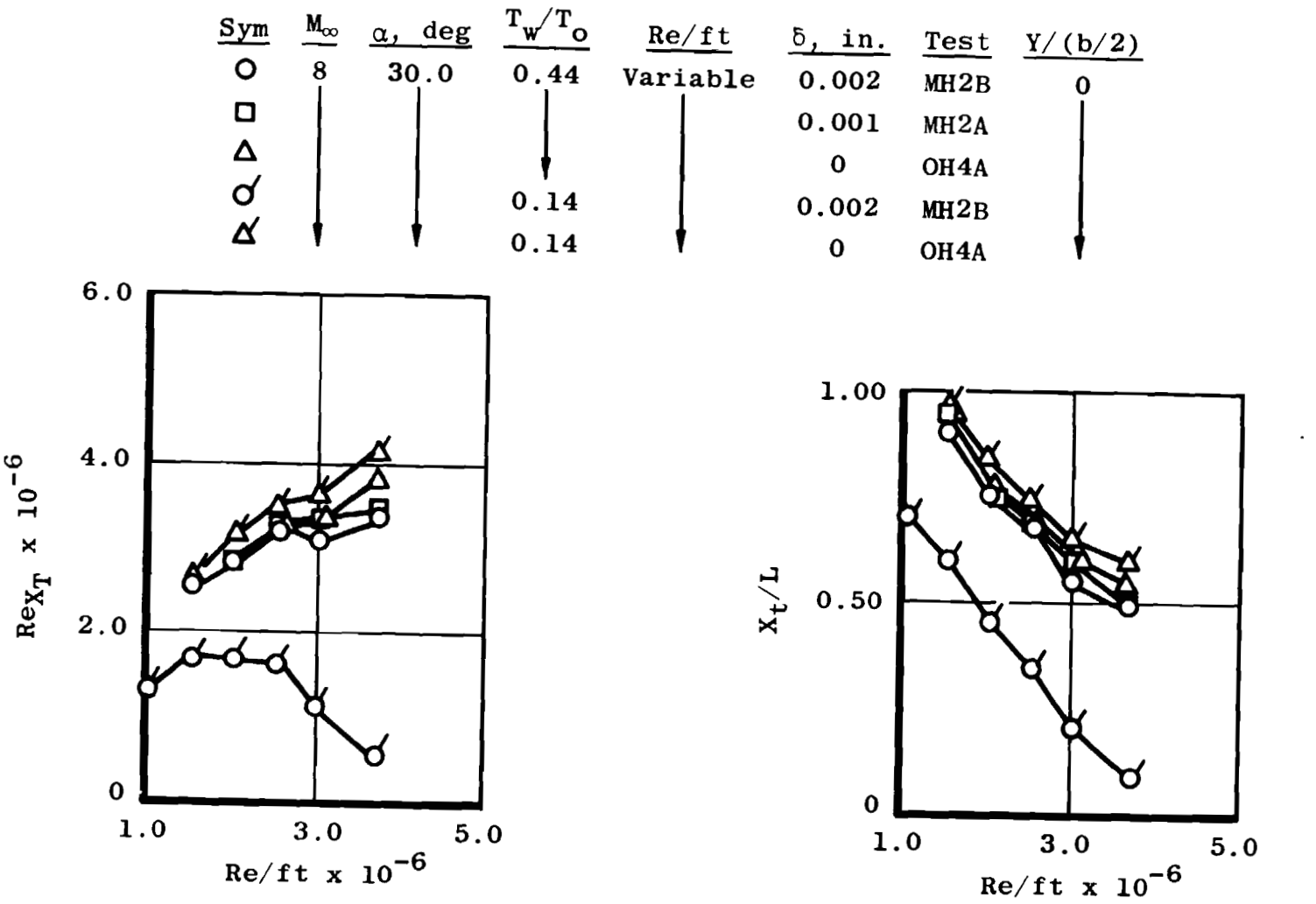

b. Surface roughness effects
Figure 11. Continued.

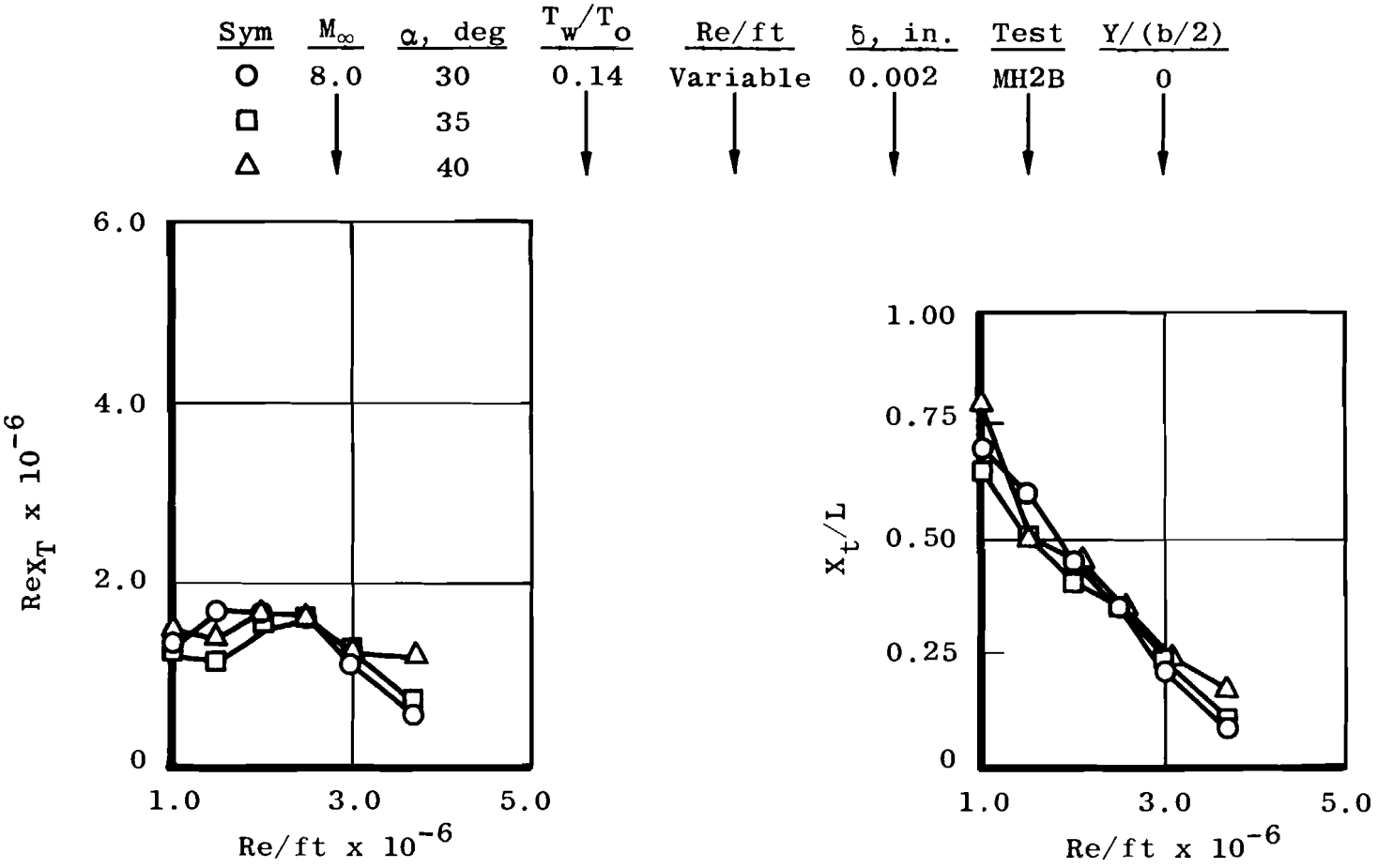

c. Angle-of-attack effects
Figure 11. Concluded.

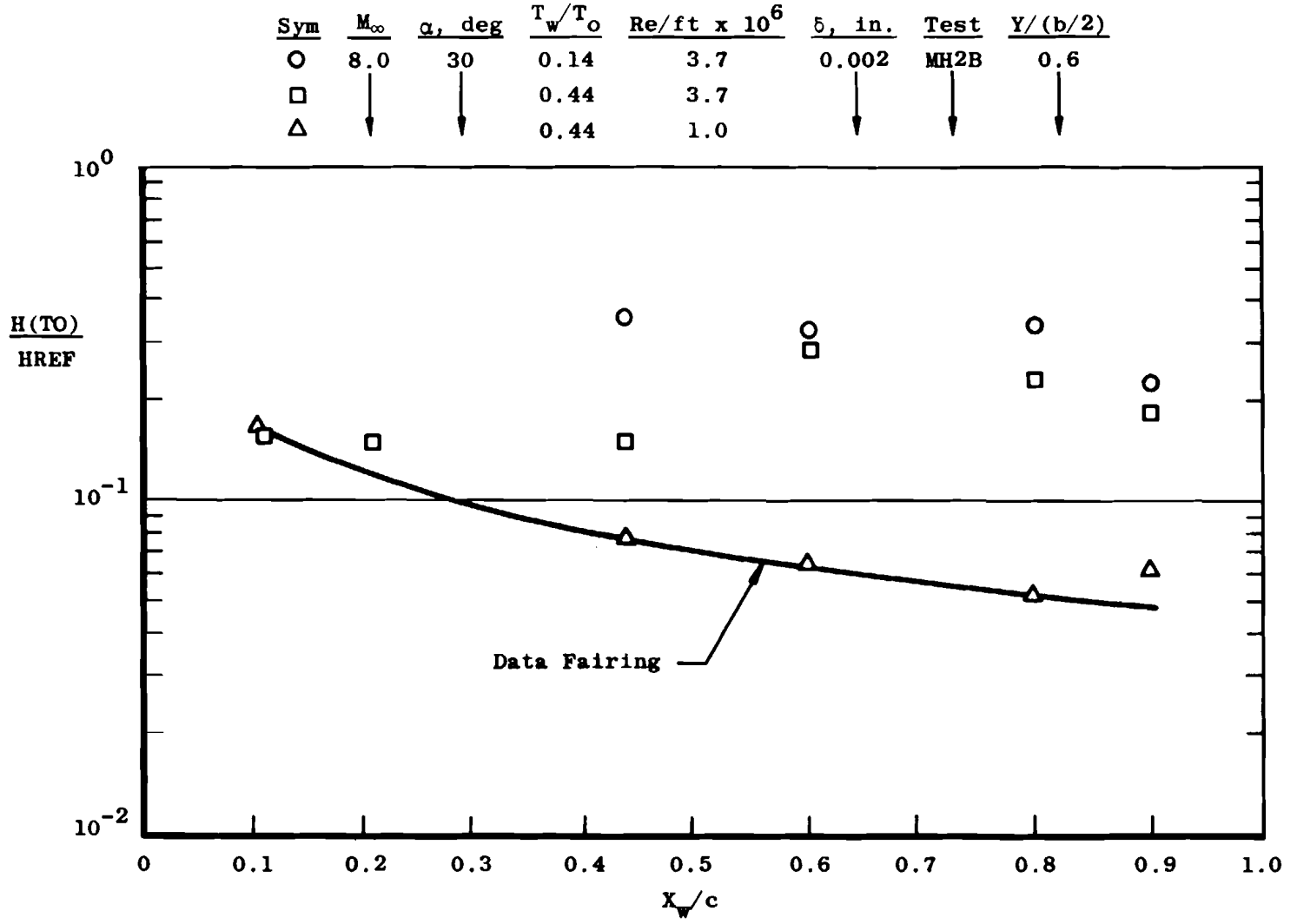

Figure 12. Temperature effect at 60-percent semispan location.

Table 1. Gage Locations

Gage No.	X, in.	ϕ, deg	Y, in.	X/L	Y/(b/2)
1	0.113	0	0	0.005	0
2	0.452			0.020	
3	0.903			0.040	
6	1.355			0.060	
7	1.806			0.080	
8	2.258			0.100	
10	3.387			0.150	
11	3.387	20	---		---
12	3.387	30	---		---
13	3.387	45	---		---
16	4.516	0	0	0.200	0
17	4.516	---	0.875	0.200	0.107
19	5.080	0	0	0.225	0
20	5.645			0.250	
22	6.209			0.275	
23	6.774			0.300	
24	6.774	34	---		---
25	6.774	40	---		---
26	6.774	45	---		---
29	7.339	0	0	0.325	0
30	7.898		0	0.350	
31	9.032		0	0.400	
32	9.032	---	0.875	0.400	0.107
33	10.161	0	0	0.450	0
34	11.290		0	0.500	0
35	11.290		0.875	0.500	0.107
37	12.419		0	0.550	0
38	13.548		0	0.600	0
39	13.548	---	0.875	0.600	0.107
40	14.677	0	0	0.650	0
41	15.806			0.700	
43	16.935			0.750	
44	18.064			0.800	
45	18.064	---	0.875	0.800	0.107
46	19.193	0	0	0.850	0
47	20.322	0	0	0.900	0
48	20.322	---	0.875	0.900	0.107
49	21.451	0	0	0.950	0
50	22.580	0	0	1.000	0

Table 1. Concluded

Gage No.	X, in.	Y, in.	$X_{w/c}$	Y/(b/2)
52	9.032	2.049	0.082	0.250
53	11.290	2.049	0.302	↓
54	13.548	2.049	0.447	↓
55	15.806	2.049	0.591	↓
56	18.064	2.049	0.736	↓
57	20.322	2.049	0.881	↓
59	14.022	3.278	0.10	0.4
60	14.910	↓	0.20	↓
61	15.806	↓	0.30	↓
62	18.064	↓	0.56	↓
63	19.307	↓	0.70	↓
64	21.066	↓	0.90	↓
65	15.806	4.098	0.176	0.50
66	18.064	↓	0.484	↓
82	19.618	↓	0.702	↓
67	21.076	↓	0.90	↓
68	15.995	4.918	0.10	0.60
69	16.625	↓	0.20	↓
70	18.064	↓	0.43	↓
71	19.145	↓	0.60	↓
72	20.405	↓	0.80	↓
73	21.035	↓	0.90	↓
74	17.084	6.147	0.10	0.75
75	18.064	↓	0.30	↓
76	19.022	↓	0.50	↓
77	19.117	↓	0.70	↓
78	20.961	↓	0.90	↓
79	17.801	6.967	0.10	0.85
80	18.578	↓	0.30	↓
81	19.355	↓	0.51	↓

Table 2. Test Summary

α, deg	T_w/T_o	Re/ft x 10^6						
		0.5	1.0	1.5	2.0	2.5	3.0	3.7
30	0.44		X	X	X	X	X	X
35	↓		X	X	X	X	X	X
40	↓		X	X	X	X	X	X
30	0.34		X	X	X	X	X	X
35	↓		X	X	X	X	X	X
40	↓		X	X	X	X	X	X
30	0.24				X			X,X**
35	↓				X			X
40	↓				X			X
30	0.14	X*, X**	X	X	X	X	X	X
35	↓	X*	X	X	X	X	X	X
40	↓	X*	X	X	X	X	X	X

$M_\infty = 8.0$

* Runs with moderate model frost

** Runs with heavy model frost
(These data not recommended for aerodynamic analysis)

Table 3. Rockwell International SSV Trajectory No. 14,040.

Time, sec	Altitude, ft	Velocity, ft/sec	M_∞	Re/ft*
400	269,915	26,006	29.41	2,610
496	252,149	25,576	28.01	66,064
608	243,742	24,727	26.38	8,193
704	239,322	23,864	25.14	9,390
800	233,322	22,897	23.73	11,214
896	225,698	21,767	22.09	14,177
1,008	212,699	20,119	19.74	10,525
1,104	195,803	18,148	17.22	32,755
1,200	186,076	15,665	14.70	39,921
1,296	178,440	13,310	12.39	44,194

*These values cover the range of probable transition on the Orbiter centerline

NOMENCLATURE

b Total model wing span, 16.4 in.

c Local wing chord, in.

c_p Gage specific heat, Btu/lbm-°R

HREF Reference heat-transfer coefficient based on Fay-Riddel theory, Btu/ft^2-sec-°R

$$\text{HREF} = \left\{ \frac{8.139\,(P'_o)^{0.5}\,(\mu_o)^{0.4}\,[1-(p_\infty/P'_o)]^{0.25}}{(r_n)^{0.5}\,(T_o)^{0.15}} \right\} \times [0.2235 + 0.0000135(T_o + 560)]$$

where

P'_o = stagnation pressure downstream of a normal shock, psia

μ_o = air viscosity based on T_o, lbf

r_n = reference nose radius, (0.0175 ft)

p_∞ = free-stream static pressure

H(TO) Heat-transfer coefficient, $\dot{q}/(T_o - T_w)$, Btu/ft^2-sec-°R

k Gage thermal conductivity, Btu/ft-sec-°R

L Model centerline length, 22.58 in.

M_∞ Free-stream mach number

P_o Tunnel stilling chamber pressure, psia

$\dot{q}(t)$ Heat-transfer rate, Btu/ft^2-sec

Re/ft Free-stream Reynolds number per foot, ft^{-1}

Re_{X_t} Free-stream Reynolds number based on distance from model nose to beginning of transition

$\overline{T}$ $T_w - T_{w_i}$

T_o Free-stream stagnation temperature, °R

T_w Gage surface temperature, °R

T_{w_i} Gage surface temperature at initial time, °R

t Time, sec

X Longitudinal coordinate, in. (see Fig. 2)

X_t Longitudinal location of beginning of transition, in.

X_w Longitudinal coordinate with origin at wing leading edge, in. (see Fig. 2)

Y Lateral coordinate, in. (see Fig. 2)

α Model angle of attack, deg

δ TPS tile misalignment height, in.

ϕ Thermocouple orientation angle in the cross-sectional plane of the Oribter, deg (see Fig. 2)

ρ Gage density, lbm/ft^3